# Influence of thermophysical properties of working fluid on the design of cryogenic turboexpanders using $n_s$-$d_s$ diagram


**Ashish Alex Sam, Parthasarathi Ghosh**

Cryogenic Engineering Centre

Indian Institute of Technology Kharagpur, India



## Abstract

Cryogenic turboexpanders are an essential part of liquefaction and refrigeration plants. The thermodynamic efficiency of these plants depends upon the efficiency of the turboexpander, which is the main cold generating component of these plants and therefore they should be designed for higher thermodynamic efficiencies. Balje's $n_s$–$d_s$ chart, which is a contour of isentropic efficiencies plotted against specific speed ($n_s$) and specific diameter ($d_s$) is commonly used for the preliminary design of cryogenic turboexpanders. But, these charts were developed based on calculations for a specific heat ratio (ϒ) of 1.4, and studies show that care should be taken while implementing the same for gases which has higher ϒ of 1.67. Hence there is a need to investigate the extent of applicability of $n_s$-$d_s$ diagram in designing expansion turbine for higher specific heat ratios. In this paper Computational Fluid Dynamics (CFD) analysis of cryogenic turboexpanders, were carried out using Ansys CFX®. The turboexpanders were designed based on the design methodologies prescribed by Kun and Sentz following the $n_s$-$d_s$ diagram of Balje and Hasselgruber's technique for generating blade profile. The computational results of the two cases were analysed to investigate the applicability of Balje's $n_s$-$d_s$ diagram for the design of turboexpanders for refrigeration and liquefaction cycles. Efforts have also been made to discern the modifications that should be made in the existing design techniques following Balje's chart so as to establish a streamlined design methodology for the development of turboexpanders with improved performance.


## Introduction

❑ The low volumetric flow rate and variation of thermophysical properties at low temperatures makes the design of a cryogenic turboexpander for liquefaction systems demanding [1].

❑ Conventional turbomachinery blade design methods includes the 1D preliminary design, which involves the use of similarity parameters ( performance charts, empirical data etc.) the 1D meanline analysis and the 2D inverse blade design procedures [2].

❑ Balje's $n_s$-$d_s$ chart (figure 1) which shows lines of optimum geometry along with contours of constant efficiency, is a widely accepted approach for the prediction of turbomachinery efficiency and for the selection of design parameters [1].

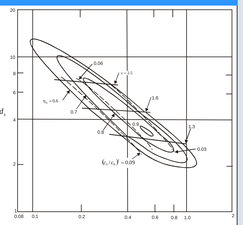


Figure 1. Balje's $n_s$-$d_s$ diagram [3].

❑ Similarity principles stipulate that machines that have the same specific speed ($n_s$), the same specific diameter ($d_s$) and similar design geometry will be dynamically equivalent and thus have the same efficiency, if Reynolds number and Mach number effects are neglected.

$$\eta = f(n_s, d_s, \text{geometrical parameters, } Re^*, La^*, \Upsilon)$$

❑ The maximum efficiency values are valid only if Re* is greater than 2 x $10^6$, La* is less than unity and geometrical similarities are maintained on clearance ratio, trailing edge ratio and surface roughness ratio [1].

❑ Macchi [4] has shown that as the Balje's $n_s$-$d_s$ diagram was obtained for a working fluid with a ϒ=1.41, the chart needs to be modified for it to be used for working fluid with higher ϒ.

## Objective

❑ To compare the performance of cryogenic turboexpanders designed for two different working fluids, one with nitrogen and the other with helium, through CFD analysis.

❑ To verify the applicability of Balje's $n_s$-$d_s$ chart for design of turboexpanders with the working fluid having a higher specific heat ratio and a low volumetric flow rate.

## Design methodology and major dimensional parameters

❑ The cryogenic turboexpander in refrigeration and liquefaction cycles constitute an inlet nozzle for guiding the flow, a 90° inward flow radial turbine and a diffuser for recovering the pressure (figure 2).

❑ The preliminary design of the turboexpanders were made based on Balje's $n_s$-$d_s$ chart and the one dimensional meanline analysis was done following Kun and Sentz' [5] design methodology [1,6].

❑The blade for turbine has been generated following methodology prescribed by Hasselgruber [7] and Balje [3]. The specifications of the turbines are presented in table 1.

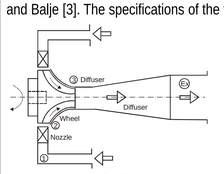


**State points:**

1: Inlet to nozzle (overall inlet)
2: Inlet to wheel (exit from nozzle)
3: Inlet to diffuser (exit from wheel)
Ex: Exit from diffuser (overall exit)

Figure 2. The fluid flow path in a turbine [1].

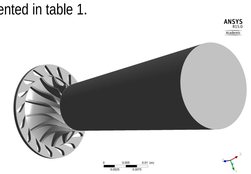


Figure 3. 3D model of turbine.

Table 1. Turboexpander specifications.

| Parameter | Nitrogen turboexpander | Helium turboexpander |
|---|---|---|
| Total pressure at inlet | 6 bar | 16.5 bar |
| Total temperature at inlet | 120 K | 70 K |
| Mass flow rate | 0.06 kg/s | 0.05 kg/s |
| Static pressure at exit | 1.5 bar | 11 bar |
| Specific speed | 0.548 | 0.587 |
| Specific diameter | 3.54 | 3.14 |
| Machine Reynolds number | 7.75 x $10^6$ > 2 x $10^6$ | 4.48 x $10^6$ > 2 x $10^6$ |
| Laval number | 0.96 < 1 | 0.52 < 1 |

## Methodology

### Geometry and grid

❑ The 3D model of the turbine wheel (figure 3) was developed using ANSYS BladeGen® and was meshed using ANSYS TurboGrid®.

❑ The inlet nozzle and the diffuser section were modelled using ANSYS DesignModeler® and ANSYS CFX-Mesh® was employed to generate the mesh (table 2).

Table 2. Mesh specifications for various components.

| Turboexpander | Domain | Number of nodes | Number of elements | Method | Mesh type/ type of elements |
|---|---|---|---|---|---|
| Nitrogen Turboexpander | Nozzle | 101728 | 78400 | Sweep | Unstructured/ mostly hexahedral, small number of wedge |
| | Turbine | 676942 | 621194 | ATM optimised | Structured (H and O type topology)/ hexahedral only |
| | Diffuser | 58557 | 321920 | Patch conforming method | Unstructured/ tetrahedral |
| Helium turboexpander | Nozzle | 154978 | 610621 | Sweep | Unstructured/ mostly hexahedral, small number of wedge |
| | Turbine | 1391193 | 1260064 | ATM optimised | Structured (H and O type topology)/ hexahedral only |
| | Diffuser | 165683 | 514713 | Patch conforming method | Unstructured/ tetrahedral |

### Boundary conditions

❑ The mass flow rate and total temperature were specified at the nozzle inlet and the static pressure was specified at the diffuser outlet.

❑ Flow regime is subsonic in nature at both inlet and outlet surface.

❑ All walls were assumed to be smooth, adiabatic and having no slip.

### Numerical model

❑ RANS equation based SST (Shear Stress Transport) model was used for turbulence modelling [8].

❑ Frozen rotor model was used for modelling the rotor stator interface [9].

❑ The Peng-Robinson cubic equation of state was used to describe the properties of nitrogen and in the case of helium, the ideal gas equation of state was employed [10].

### Convergence criteria

❑ The simulations were carried out till the residuals decreased to $10^{-4}$ (Root Mean Square) for all the conservation equations. The convergence of the solutions was ensured by monitoring the residual values and variables of interest.

## Results and Discussion

Table 3. Comparison of 1D meanline analysis and CFD analysis.

| Performance parameter | Nitrogen turboexpander | | Helium turboexpander | |
|---|---|---|---|---|
| | 1D Design value | CFD analysis | 1D Design value | CFD analysis |
| Nozzle efficiency | 93% | 97.05% | 93% | 96.46% |
| Turbine efficiency (total to static) | 75% | 77.21% | 65% | 72.28% |
| Turbine wheel efficiency (total to static) at turbine wheel exit | 75% | 75.49% | 65% | 67.31% |
| Power | 1.73 kW | 1.99 kW | 1.8 kW | 2.21 kW |
| Diffuser pressure recovery factor | 0.7 | 0.37 | 0.7 | 0.73 |

❑The nozzle efficiency from CFD analysis for both the cases are comparable with the 1D design values, whereas the turbine wheel efficiency is higher in case of helium turboexpander . The diffuser performance in case of nitrogen is poor as compared to that of helium (table 3).

❑ The velocity vector plots in figure 4, near the trailing edge, exhibits the presence of vortex flow, which is a source of entropy generation in the turboexpanders.

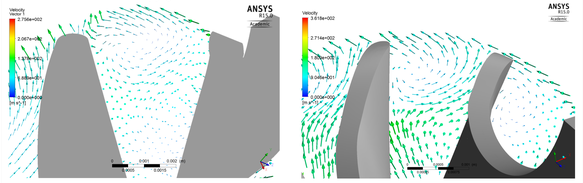


(a) (b)

Figure 4. Velocity vector plots near the trailing edge in (a) Nitrogen turboexpander and (b) Helium turboexpander.

❑ From figures 5 and 6 it can be seen that the vortex originates at the suction side near the shroud tip and as the flow propagates it gets strengthened and shifts towards the mid passage.

❑ A closer look at the entropy contour plots of the two turboexpander (figures 5 and 6) shows that the entropy generated due to the vortex flow in the helium turboexpander is higher than that in nitrogen turboexpander. This may be the result of greater tip leakage flow due to the lower viscosity of helium as compared to nitrogen.

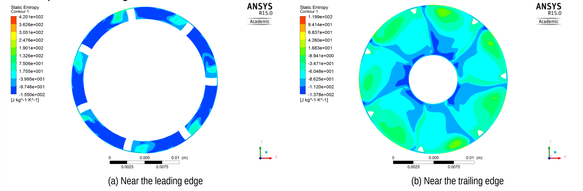


(a) Near the leading edge (b) Near the trailing edge

Figure 5. Entropy contour at different stream wise locations in nitrogen turboexpander.

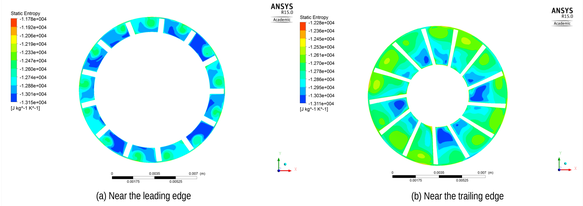


(a) Near the leading edge (b) Near the trailing edge

Figure 6. Entropy contour at different stream wise locations in helium turboexpander.

❑ The velocity vector plots in the blade to blade view nearer to the shroud tip (figure 7) shows the strong cross flow from the pressure side to the suction side of the blade through the tip clearance which leads to the formation of vortices near the leading edge.

❑ Figure 8 portraits the static entropy contours nearer to the shroud. It can be seen that the entropy generation due to tip leakage flow in helium turboexpander is higher compared to nitrogen turboexpander.

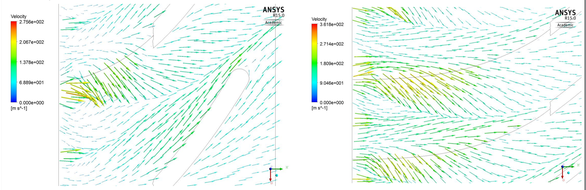


(a) Nitrogen turboexpander (b) Helium turboexpander

Figure 7. Velocity vector plots nearer to the shroud in the blade to blade view.

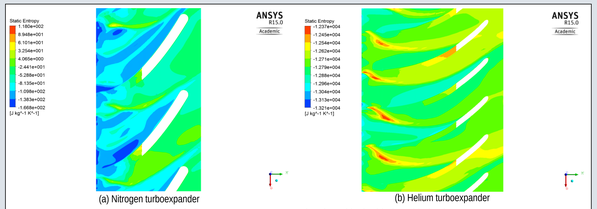


(a) Nitrogen turboexpander (b) Helium turboexpander

Figure 8. Entropy contour nearer to the shroud in the blade to blade view

❑ Figure 9 depicts the entropy generated by the trailing edge vortices. Baines [11] has shown that the sudden expansion at the rotor exit results in flow separation and formation of vortices which leads to trailing edge loss.

❑ The entropy contour reveals that the entropy generation due to trailing edge vortices in helium turboexpander is greater than that in nitrogen turboexpander.

❑ Trailing edge loss usually increases for low supersonic outflow (Mach number, M < 1.2) and for turbine with thick trailing edges.

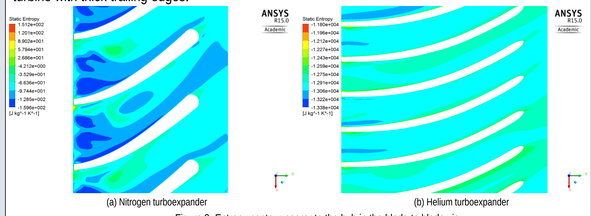


(a) Nitrogen turboexpander (b) Helium turboexpander

Figure 9. Entropy contour nearer to the hub in the blade to blade view

## Conclusion

❑ The CFD analysis of nitrogen and helium turboexpanders were performed and the results were compared with 1D design values.

❑ The analysis revealed that the entropy generation in helium turboexpander was greater as compared to that in nitrogen turboexpander. This may be due to the effect of thermophysical properties like viscosity and geometrical parameters like clearance ratio, trailing edge ratio etc.

❑ Minimization of the pressure gradient across the blade and reduction of tip leakage flow through the shroud tip clearance is possible through a modification of the blade profile and a reduction of the tip clearance height. Tip clearance height can either be kept constant or varied from the leading to the trailing edge, provided the stress and manufacturing constraints are taken into consideration.

❑ Therefore, the 1D preliminary design methodology for helium turboexpander needs to be modified by incorporating the effect of these thermophysical properties and geometrical parameters.

❑ The present study showed that there is considerable difference in the flow fields between nitrogen and helium turboexpanders that are designed based on $n_s$-$d_s$ diagram and Hasselgruber's method. The effect of ϒ on these differences will be further explored.

❑As the turbomachinery flow is highly turbulent and unsteady, transient analysis are required to completely capture the flow physics.

## Nomenclature

Nozzle efficiency, $\eta_n = (h_{0,1} - h_{0,2}) / (h_{0,1} - h_{2,s})$

Power output of the turbine, $P = \dot{m}(h_{0,1}-h_{0,2})$

Total-to-static efficiency, $\eta_{T-tt} = (h_{0,1} - h_{0,ex}) / (h_{0,1} - h_{ex,s})$

Total-to-static efficiency at the rotor exit, $\eta_{T-tt} = (h_{0,1} - h_{0,3}) / (h_{0,1} - h_{3,s})$

Diffuser pressure recovery factor, $C_p = (P_{ex} - P_3) / (P_{03} - P_3)$

## Subscripts

0 – stagnation condition
1 – inlet to the nozzle
2 – inlet to the turbine
3 – exit from the turbine wheel
ex – discharge from the diffuser
Re* - machine Reynolds number
La* - Laval number
m – mass flow rate
s – isentropic state
h – enthalpy
P – pressure

## References


1. Ghosh P 2002. Analytical and Experimental Studies on Cryogenic Turboexpander *Ph.D dissertation. IIT Kharagpur.*
2. Moustapha H, Zelesky M F, Baines N C and Japikse D 2003 Axial and Radial Turbines *Concepts NREC.*
3. Balje O E 1981 Turbomachines *John Wiley and Sons.*
4. Macchi E 1985 Design limits, basic parameter selection and optimization methods in turbomachinery design *Thermodynamics and Fluid Mechanics of Turbomachinery* 2 805-828.
5. Kun L C and Sentz R N 1985 High efficiency expansion turbines in air separation and liquefaction plants *Beijing, China Int. Conf. on Production and Purification of Coal Gas & Separation of Air* 1 – 21.
6. Ghosh S K 2010 A numerical model for the design of a mixed flow cryogenic turbine *Int. J. Eng. Sci. and Tech.* 2(1) 175–91.
7. Hasselgruber H 1958. Stromungsgerechte gestaltung der laufrader von radialcompressoren mit axialem laufradeintritt Konstruction10 (1) 22 (in German).
8. Menter F R 2009 Review of the shear-stress transport turbulence model experience from an industrial perspective. *Int. J. of Computational Fluid Dynamics* 23 (4) 305-316.
9. Brost V Ruprecht, A and Maihofer M 2003 Rotor-stator interactions in an axial turbine, a comparison of transient and steady state frozen rotor simulations *Belgrade Conf. on case studies in hydraulic systems.*
10. Thomas R J, Dutta R Ghosh P and Chowdhury K, Applicability of equations of state for modeling helium systems. *Cryogenics* 52(7-9) 375–81.
11. Baines N C 1998 A meanline prediction method for radial turbine efficiency. *Inst. Mech. Eng. Conf. on Turbochargers. IMechE (UK) Publications.*



CEC-ICMC 2015 : Track : CEC – 05 : I.D : C3PoE : 27